View Factor Model and Validation for Bifacial PV and Diffuse Shade on Single-Axis Trackers

Marc Abou Anoma[1], David Jacob[1], Ben C. Bourne[1], Jonathan A. Scholl[1], Daniel M. Riley[2], Clifford W. Hansen[2]

[1]SunPower Corporation, San Jose, CA, 95134, USA
[2]Sandia National Laboratories, Albuquerque, NM, 87185, USA

***Abstract* — In this paper, we use a model based on view factors to estimate the irradiance incident on both surfaces of a single-axis tracker PV array for given direct and diffuse light components of the sky dome. We describe the mathematical formulation of the view factor model that assumes a 2D tracker geometry with Lambertian surfaces while accounting for reflections from all surrounding surfaces. The model allows specifically to calculate the incident irradiance on the back surface of PV modules as well as the diffuse shading effects caused by the presence of neighboring tracker rows in a PV array. We present preliminary results on an experimental validation of the view factor model.**

I. Introduction

Due to new bifacial technologies and larger utility-scale photovoltaic (PV) arrays, there is a growing need for models that can more accurately account for the multiple diffuse light components and reflections incident on various surfaces of a PV array. The literature shows the use and validation of ray-tracing methods and view factors on 3D geometries to calculate back-surface irradiance on PV modules [1]. View factors have also been used to account more accurately for diffuse light and ground reflections incident on the front surface of PV module 3D geometries [2]-[3]. These methods have been shown to be quite accurate under careful management of the calculation, but they can often be computationally intensive and complex to use.

The method presented here is an application of view factors for a 2D geometry of an array of single-axis trackers, invariant by translation along the tracker axis. It can be used for energy production calculation of large PV arrays thanks to its high computational speed, and also because edge effects occurring in large PV arrays are negligible. We present preliminary work on the experimental validation of this method and show encouraging results.

Calculating view factors for 2D geometries is straightforward and formulas for a large amount of geometries have already been derived and published in the literature [4]. The present work makes use of these formulas, applies them to a geometry in an analytically derived mathematical formulation and enables the calculation of the incident irradiance on all surfaces of the considered 2D geometry while accounting for reflections from all surfaces.

We show that the method is in good agreement with measurements of back-over-front surface irradiance ratio on single-axis trackers installed at a Sandia National Laboratories test site in Albuquerque, New Mexico. We also present preliminary results on how this work can be combined with a diffuse transposition model such as the Perez model [5] to account more accurately for ground reflections as well as shading of diffuse light. Lastly, we compare the model with measurements performed on single-axis trackers installed at the SunPower R&D Ranch located in Davis, California.

II. Model Description

In a PV array of modules, neighboring rows have an impact on the irradiance incident on the front and the back surface of PV modules because of the portion of the sky and the ground they obstruct. They also reflect some light and cast shadows on the ground. We illustrate in Fig. 1 the main components of irradiance on a tracker and show the effects of diffuse shading between neighboring trackers and ground reflection.

This work shows how these effects can be captured using view factors on a 2D model of a PV array, when applied in conjunction with a mathematical model for reflections, and optionally with an existing transposition model such as the Perez model [5].

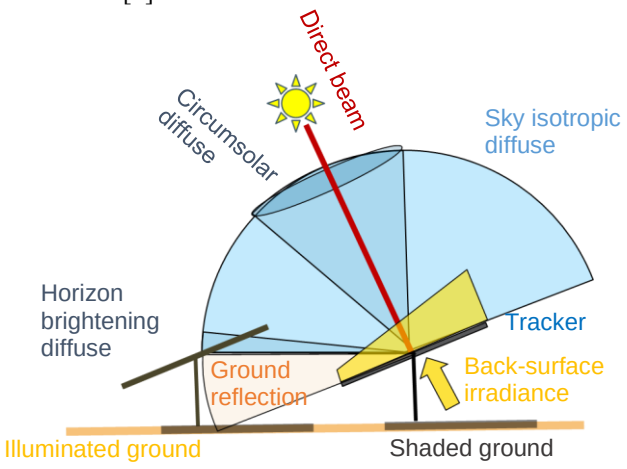

Fig. 1. Schematic showing a 2D representation of a PV array and the effects of neighboring rows on incident irradiance components on the front and back surface of modules. The left tracker obstructs a portion of the sky and casts a shadow on the ground that decreases the reflected irradiance seen by the right tracker.

A. View Factors

View factors, also called configuration factors, are extensively used in thermal radiation heat transfer theory. The view factor from a surface 1 to another surface 2 represents the fraction of the space surrounding and seen by surface 1, and occupied by surface 2.

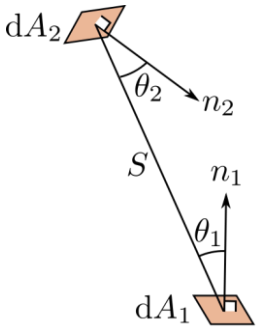

$$F_{1,2} = \frac{1}{A_1}\int_{A_1}\int_{A_2}\frac{cos\theta_2\ cos\theta_1}{\pi\ S^2}\ dA_2\ dA_1 \qquad (1)$$

The present method relies on analytical solutions of view factors that have already been calculated and published for 2D geometries [4]. In a 2D-geometry, surfaces are modeled by segments in the same plane. Doing so helps improve the computational speed of the model.

B. Model equations

By making several simplifying assumptions on the modeled PV array surfaces, we can represent the irradiance calculation of a modeled array with a linear system of equations. The dimension of the system is equal to the number of surfaces considered, n. For a surface of index i (integer from 1 to n), we can write that:

$$q_{o,i} = q_{emitted,i} + q_{reflected,i} \qquad (2)$$

where $q_{o,i}$ is the radiosity of surface i, representing the outgoing radiative flux from i. We can write this equation for all n surfaces, and recognize that they are all coupled because surfaces reflect and emit to each other in a PV array. Therefore, we must find all the radiosity terms of all surfaces in order to solve the system and to calculate values of interest like back-surface incident irradiance for instance.

If we assume that the emitted thermal power $q_{emitted,i}$ is negligible compared to $q_{reflected,i}$, we can simplify (2):

$$q_{o,i} \approx q_{reflected,i} \qquad (3)$$

This assumption is reasonable because the temperature of the modules in the field, around 50-60°C, is associated to the emission of much lower energy photons than the photons in the visible spectrum reflected by the surfaces. Assuming Lambertian surfaces we can write that:

$$q_{reflected,i} = \rho_i * q_{incident,i} \qquad (4)$$

where ρ_i is the albedo of surface i. We can further develop (4) into:

$$q_{reflected,i} = \rho_i * (\sum_j q_{o,j} * F_{i,j} + Irradiance_i) \qquad (5)$$

where:

- $\sum_j q_{o,j} * F_{i,j}$ is the contribution of all the surfaces j surrounding i to the incident radiative flux onto surface i. For instance, this could be the irradiance contributions of the sky dome, the ground surfaces and the other trackers to the front surface of a PV module.
- $F_{i,j}$ is the view factor of surface i to surface j.
- $Irradiance_i$ is an irradiance source term specific to surface i, and which includes irradiance contributions from sources not considered to be surfaces in the modeled system. In this work, for instance, it can be equal to the sum of direct, circumsolar, and horizon light components incident on the front surface of the modeled PV modules.

After accounting for the radiosity terms of all the surfaces, we get a system of n coupled equations and can solve it to calculate values of interest such as back-surface incident irradiance. The system of equations indicated by (5) can be written as:

$$(\mathbf{R^{-1}} - \mathbf{F}).\mathbf{q_o} = \mathbf{Irr} \qquad (6)$$

or more explicitly:

$$\left[\begin{pmatrix}\rho_1 & 0 & 0 & \cdots & 0\\ 0 & \rho_2 & 0 & \cdots & 0\\ \vdots & \vdots & \vdots & \ddots & \vdots\\ 0 & 0 & 0 & \cdots & \rho_n\end{pmatrix}^{-1} - \begin{pmatrix}F_{1,1} & F_{1,2} & F_{1,3} & \cdots & F_{1,n}\\ F_{2,1} & F_{2,2} & F_{2,3} & \cdots & F_{2,n}\\ \vdots & \vdots & \vdots & \ddots & \vdots\\ F_{n,1} & F_{n,2} & F_{n,3} & \cdots & F_{n,n}\end{pmatrix}\right].\begin{pmatrix}q_{o,1}\\ q_{o,2}\\ \vdots\\ q_{o,n}\end{pmatrix} = \begin{pmatrix}Irr_1\\ Irr_2\\ \vdots\\ Irr_n\end{pmatrix} \qquad (7)$$

In order to solve this system for $\mathbf{q_o}$ we provide values for the reflectivity and the irradiance term of each surface, and calculate the view factors from each surface to the other surfaces. The vector of incident irradiance on all surfaces $\mathbf{q_{incident}}$ can then be calculated using:

$$\mathbf{q_{incident}} = \mathbf{F}.\mathbf{q_o} + \mathbf{Irr} \qquad (8)$$

C. Application to a 2D PV array of single-axis trackers

In this work, we implemented a geometrical model of a 2D PV array of single-axis trackers using the programming language Python.

After specifying key geometric and environmental inputs such as tracker height, width, and spacing, the algorithm builds a simple 2D geometry representing a PV array with an arbitrary number of rows and their shadows on the ground at a single point in time for which we specify the solar and tracker angles. We built a logic into the algorithm that enables each surface to detect the other surfaces surrounding it, as shown in Fig. 1 and

Fig. 2. The algorithm also allows to divide some surfaces into smaller segments in order to evaluate irradiance distributions.

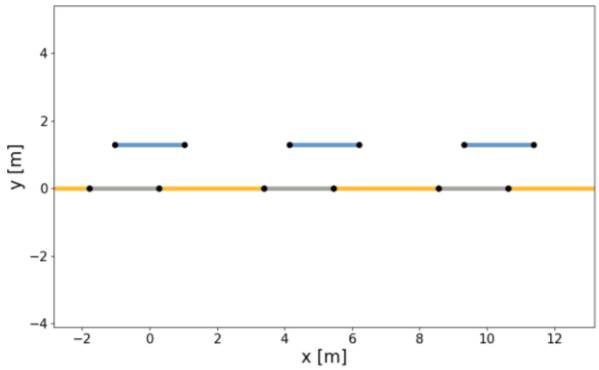

Fig. 2. Python representation of a 2D PV array of three single-axis trackers in a flat position. The three top lines represent the trackers, and the lines underneath represent the shadows (grey) and the illuminated ground (yellow). In this situation, the trackers are north-south oriented and the sun is in the east with a zenith angle of 30°.

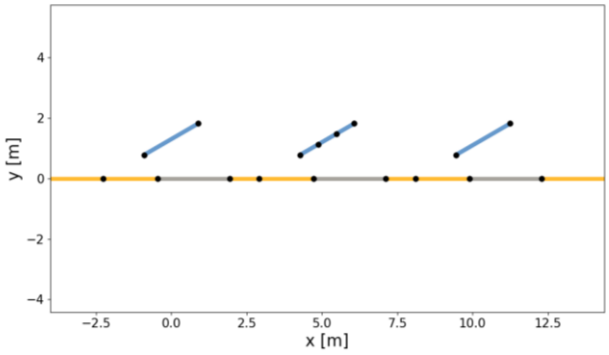

Fig. 3. Python representation of a 2D PV array of three north-south oriented single-axis trackers at 30° rotation angle, with the sun located in the west at a zenith angle of 30°. The surface of the middle tracker has been discretized into three surfaces in order to calculate the irradiance distribution on it.

The integration of both geometrical and mathematical models provides a fast way to calculate the incident irradiance on all defined surfaces after providing the solar and tracker angles with the direct and diffuse light intensities.

III. Validation and Preliminary Results

In this section, we use the view factor algorithm described above to calculate the irradiance on north-south oriented single-axis trackers installed at Sandia National Laboratories in New Mexico and at the SunPower R&D Ranch in California.

In addition, we use the pvlib Python [6] implementation of the Perez model [5] to calculate the direct, circumsolar, and horizon plane-of-array (POA) and ground irradiance components, as well as the luminance of the isotropic sky dome. These pre-calculated components allow the view factor model (VF model) to calculate ground and tracker reflections as well as isotropic diffuse light incident on all surfaces.

A. Bifacial irradiance results

We first compare the modeled front and back surface irradiances to measurements done on two north-south oriented single-axis trackers installed at a Sandia bifacial test site in New Mexico, over a ground with an albedo close to 22% on average. Both east and west trackers have reference cells installed in the plane-of-array (POA) that measure the front and back surface irradiances.

In Fig. 4 we show one clear day dataset, with irradiance levels, tracking angles, and the back-to-front surface irradiance ratios for the two trackers.

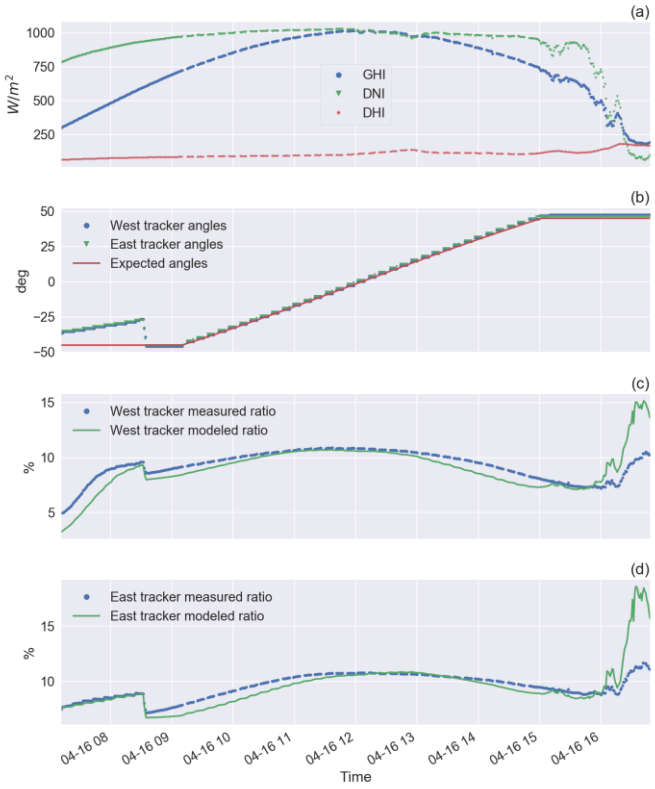

Fig. 4. Comparison of measured and modeled back to front surface irradiance ratios for two single-axis trackers installed at Sandia (NM) on a clear day with good tracking. (a) Measured irradiance at the site. (b) Measured and expected tracker angles. Angles are positive when trackers are facing west. (c) Measured and modeled back to front surface irradiance ratio of west tracker. (d) Measured and modeled back to front surface irradiance ratio of east tracker.

We observe that there is a very good agreement between the measured and modeled irradiance ratios; they remain within 2% over the course of the day during the tracking period, except at the very end of the day when clouds near the horizon and shading from nearby structures reduce the irradiance on upward facing instruments.

In Fig. 5 we show the back-surface irradiance for the two tracker rows and compare it to the model.

Fig. 5. Comparison of measured and modeled back-surface irradiance for two single-axis trackers installed at Sandia (NM) on a clear day with good tracking. (a) West tracker. (b) East tracker.

We first note that the irradiance trends predicted by the model are following the measurements within 10 W/m^2 and that the model is able to distinguish the east and the west trackers. This shows that the model accounts well for the presence of neighboring trackers.

In Fig. 6, we report the modeled contributions of the two main irradiance components on the back-surface irradiance: the irradiance that comes directly from the isotropic sky and the irradiance reflected on both the ground underneath the tracker and the neighboring tracker.

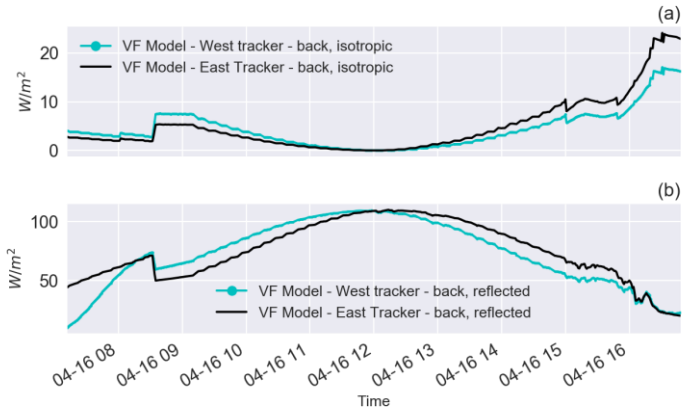

Fig. 6. Back-surface diffuse light components modeled with the view factor model for two single-axis trackers installed at Sandia (NM) on a clear day with good tracking. (a) Isotropic component. (b) Reflected component (ground and trackers).

This result shows that reflections off the ground and the trackers represent the largest contribution to the back-surface irradiance for that site. Additionally, the model accounts well for the sky shading of the east tracker in the morning by the west tracker (Fig. 6a). It also sees the shadow cast by both trackers on the ground, which causes lower intensity of incident reflected light compared to the west tracker (Fig. 6b). This trend is opposite between the two trackers in the afternoon hours.

In Fig. 7, we present results for multiple semi-clear days at the site. Looking at the difference between measured and modeled back-to-front irradiance ratios, we can see that the trends are similar.

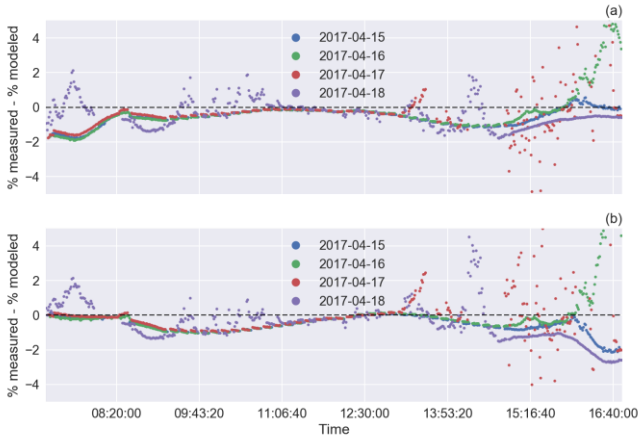

Fig. 7. Comparison of measured and modeled back-to-front surface irradiance ratios for two single-axis trackers installed at Sandia (NM) on several days. (a) Difference between measured and modeled ratio for the west tracker. (b) Difference between measured and modeled ratio for the east tracker.

These results prove that using view factors with 2D geometries allows to get fast and accurate estimates of bifacial irradiance ratios for single-axis trackers with small edge-effects.

B. Diffuse shading results

We now evaluate the ability of the view factor method to calculate the effect of diffuse shading on surfaces. In the presence of neighboring trackers, the view factor of the front surface to the diffuse sky is not only reduced compared to a free-standing tracker, but there can also be a non-uniform irradiance distribution on the front surface because of differences in view factors of the individual segments of the tracker. In a situation such as the one shown in Fig. 3, the cells on the top of the tracker have a higher view factor to the sky but a lower view factor to the ground than the bottom cells. A non-uniform illumination can be a source of current mismatch within PV strings.

1) Experimental setup

We collect diffuse shade measurements on two north-south oriented single-axis trackers installed with a ground coverage ratio close to 40% at the SunPower R&D Ranch in California. We measure the irradiance in the front plane-of-array using SunPower split-cell reference cells at four locations along the width of the west tracker (Fig. 8). This allows us to measure the distribution of irradiance on the front surface of the PV modules.

Fig. 8. Picture showing the setup of reference cells installed along the width of the west single-axis tracker at the SunPower R&D Ranch in California.

Due to site obstructions on the west side of the trackers, we are constrained to studying only data in the morning for the irradiance distribution comparisons with our model.

In Fig. 9, we present reference cell irradiance measurements taken during a clear day. They demonstrate the non-uniform irradiance distribution along the width of the tracker: we observe relative differences ranging from 3% to -3% during the course of the day between the outermost reference cells in the east and west. This relative difference changes sign during the day as the reference cells switch positions, suggesting that the top reference cell receives more irradiance than the bottom reference cell at our site.

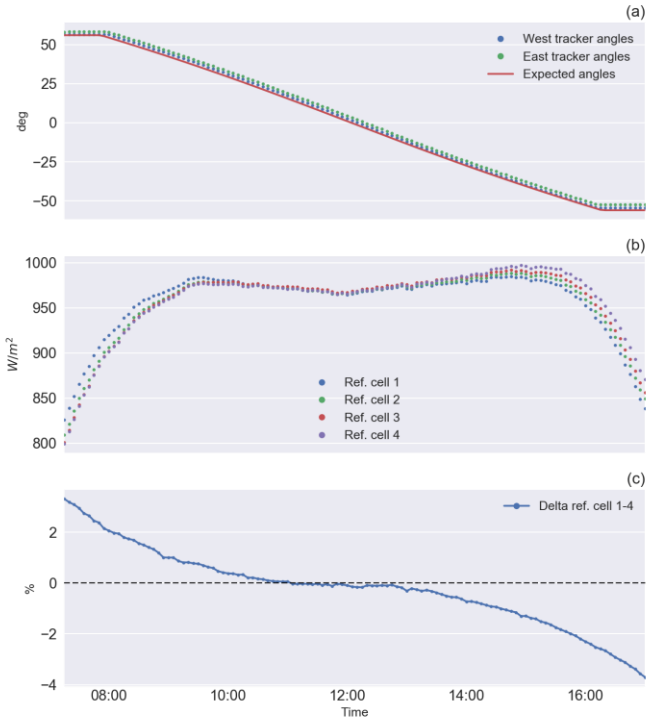

Fig. 9. Measured data from two north-south oriented single-axis trackers installed at the SunPower R&D Ranch in California, on 5/28/2017. (a) Measured and expected tracker angles. Angles are positive when trackers are facing east. (b) Irradiance measurements of reference cells installed along the width of the west tracker's front surface, where the label 1 is for the westernmost ref. cell, and the label 4 for the easternmost one. (c) Relative difference between the irradiance measurements of the two edge reference cells (1 and 4).

2) Average diffuse shading model

In our model, we assumed a site albedo of 15%, and we discretized the front surface of the modeled west tracker in order to calculate the irradiance distribution across the width of the tracker. Note that the average irradiance of the discretized irradiance segments is equal to the irradiance modeled without discretizing of the surface.

In Fig. 10 we plot the average front surface irradiance modeled with the view factor model (combined with Perez pre-calculated components) and the front surface irradiance calculated with the pvlib implementation of the Perez model [6]. The first predicts less front surface POA irradiance than the Perez model in the morning for the west tracker, because the first accounts for isotropic diffuse shading and shadows on the ground. In the afternoon, the view factor model estimates the same irradiance as the Perez model because the west tracker has no more obstructions in front of it. The two models are within 5% of the experimental irradiance curves.

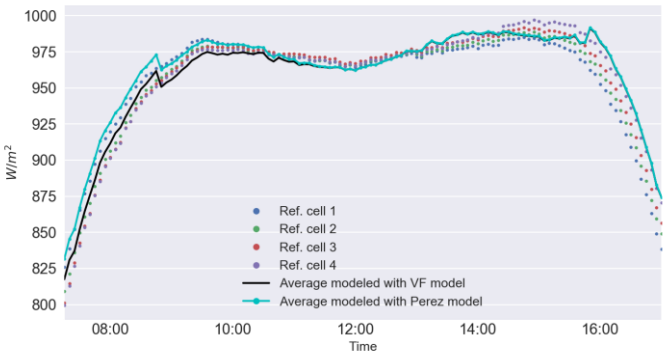

Fig. 10. Comparison of front surface total POA irradiance measured and modeled for the west single-axis tracker installed at the SunPower R&D Ranch, on 5/28/2017.

3) Modeled POA irradiance distribution

We finally present the irradiance non-uniformity modeled with a discretized tracker. In Fig. 11 we show the total irradiance, the relative difference between the two extreme segments, and the two components of irradiance responsible for the non-uniformity: the isotropic sky and the ground reflection.

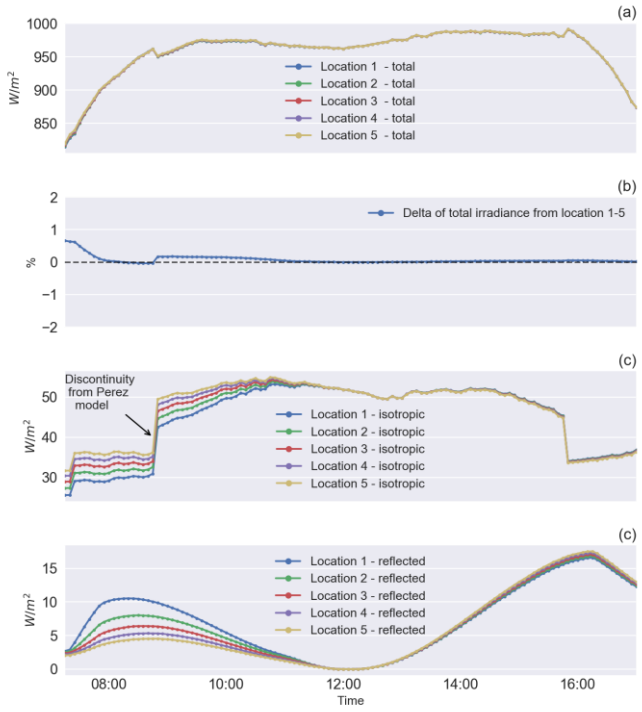

Fig. 11. Modeled diffuse shading effects for the west single-axis tracker installed at the SunPower R&D Ranch. Location 1 is the easternmost segment of the tracker, and location 5 the westernmost segment. (a) Total irradiance modeled for each location. (b) Delta between total irradiance modeled for location 5 and 1. (c) Modeled isotropic light incident on all five locations of the front surface of the tracker. The discontinuity comes from the use of the Perez model in pvlib for the isotropic luminance calculation. (d) Modeled reflected light incident on all five locations of the front side.

The model does not predict the same trend observed experimentally in the morning (Fig. 9c). According to the model, the differences in isotropic and reflected irradiances vary in opposite directions and compensate each other: the bottom segment sees more ground reflected irradiance and less isotropic sky irradiance, and vice versa for the top segment. This discrepancy could have several origins: the ground reflectivity is not broad band [7], resulting in lower reflected ground irradiance measured by the silicon-detector, the reference cells have a different Incidence Angle Modifier [8] compared to the perfect cosine detector assumed by the model, and also, circumsolar and horizon diffuse light shading should play a big role in the measured data, but is not yet implemented in the model. Further refinements of the model could help improve the agreement with the experimental results.

VI. Conclusion

A new 2D model relying on view factors and accounting for reflections and diffuse shading is presented as a computationally-efficient method for the calculation of incident irradiance on surfaces of large PV arrays of single-axis trackers. The first results on bifacial back-to-front irradiance ratios are promising, with agreement between model and experiments better than 2% for clear days. Preliminary results on the discretization of surfaces are presented to study the non-uniformities of irradiance. Further development of the model will be performed to improve the agreement between the 2D view factor model and the PV array measured data.

References

[1] Hansen, C. W., Stein, J. S., Deline, C., MacAlpine, S., Marion, B., Asgharzadeh, A., & Toor, F. (2016, June). "Analysis of irradiance models for bifacial PV modules". In Photovoltaic Specialists Conference (PVSC), 2016 IEEE 43rd (pp. 0138-0143). IEEE.

[2] Capdevila, H., Herrerías, M., & Marola, A. (2014). Anisotropic Diffuse Shading Model for Sun-tracking Photovoltaic Systems. Energy Procedia, 57, 144-151.

[3] Peled, A., & Appelbaum, J. (2016). Minimizing the current mismatch resulting from different locations of solar cells within a PV module by proposing new interconnections. Solar Energy, 135, 840-847.

[4] Howell, J. R., Menguc, M. P., & Siegel, R. (2010). Thermal radiation heat transfer. CRC press.

[5] Perez, R., Seals, R., Ineichen, P., Stewart, R., & Menicucci, D. (1987). A new simplified version of the Perez diffuse irradiance model for tilted surfaces. Solar energy, 39(3)

[6] Holmgren, W. F., Andrews, R. W., Lorenzo, A. T., & Stein, J. S. (2015, June). Pvlib python 2015. In Photovoltaic Specialist Conference (PVSC), 2015 IEEE 42nd (pp. 1-5). IEEE.

[7] Brennan M.P, A.L.Abramase, R.W.Andrewsc & J.M.Pearce (2014). Effects of spectral albedo on solar photovoltaic devices, Solar Energy Materials and Solar Cells, vol. 124

[8] Winter, S., D. Friedrich, and T. Gerloff. "Effect of the angle dependence of solar cells on the results of indoor and outdoor calibrations." Proceedings of the 25th European Photovoltaic Solar Energy Conference. 2010.